Indian J Phys (October 2019) 93(10):1345–1351
https://doi.org/10.1007/s12648-019-01397-8

ORIGINAL PAPER

Evaluation of the nuclear excitation functions of fast neutron-induced reactions on ^{52}Cr and ^{56}Fe isotopes

A Gandhi[1]*, N K Rai[1], P K Prajapati[1], B K Nayak[2], A Saxena[2], B J Roy[2], N L Singh[3], S Mukherjee[3], Y N Kopatch[4], I N Ruskov[4,5], D N Grozdanov[4,5], N A Fedorov[4,6] and A Kumar[1]

[1]Department of Physics, Banaras Hindu University, Varanasi 221005, India

[2]Nuclear Physics Division, Bhabha Atomic Research Centre, Mumbai 400085, India

[3]Department of Physics, Maharaja Sayajirao University of Baroda, Vadodara 390002, India

[4]Joint Institute for Nuclear Research, Joliot-Curie 6, Dubna, Russia 141980

[5]Institute for Nuclear Research and Nuclear Energy, 1784 Sofia, Bulgaria

[6]Moscow Lomonosov State University, Lenin Hills 1, Moscow, Russia 119991

Received: 20 August 2018 / Accepted: 05 December 2018 / Published online: 8 February 2019

Abstract: In this article, we present the nuclear excitation functions of the fast neutron-induced reactions ^{52}Cr(n,p)^{52}V, ^{52}Cr(n,α)^{49}Ti, ^{52}Cr(n,2n)^{51}Cr, ^{56}Fe(n,p)^{56}Mn, ^{56}Fe(n,α)^{53}Cr, and ^{56}Fe(n,2n)^{55}Fe, because these measurements are critical to estimate the level of the neutron activation for the fusion reactor structural materials. The theoretical computer codes TALYS-1.8 and EMPIRE-3.2.2 have been used for the calculation of the excitation functions. The theoretical calculations consider different nuclear reaction models, level density models and optical model potentials. The calculated excitation function results are compared with the existing experimental data obtained from the IAEA-EXFOR database, as well as with those available in the TENDL-2017 and ENDF/B-VIII.0-evaluated nuclear data libraries. The obtained results show the variation in excitation functions for different level density models. Moreover, we have studied the contribution from different reaction mechanisms in total reaction cross-section which varies with the incident neutron energy. These excitation function results can be useful to estimate the important parameters of nuclear reactors, such as nuclear heating, nuclear transmutation rates, and waste management etc. This kind of information can enhance the basic understanding of the mechanism of the fast neutron-induced nuclear reactions.

Keywords: Fusion reactors; Low-activation materials; Excitation functions; (n,p), (n,α), and (n,2n) reactions; TALYS-1.8; EMPIRE-3.2.2

PACS Nos.: 24.10.−i; 28.20.−v; 28.52.−s

1. Introduction

The neutron-induced nuclear reaction cross-sectional data are the vital parameter for the nuclear reactors. It shows the probability of the interaction at various neutron energies with the nuclei of the materials, through which the neutrons pass. The excitation functions of fast neutron-induced (n,p) and (n,α) reactions are needed for the estimation of hydrogen and helium gases produced in the first wall of fusion reactors because these gases cause the micro-structural defects and decrease the usability time of materials used. In addition, the (n,p), (n,α), and (n,2n) reactions data are important for designing, evaluation and construction of the nuclear reactors [1]. The cross-sectional data are also important to test the viability of the nuclear reaction theoretical model codes. The isotopes of Chromium (Cr) and Iron (Fe) elements are used in the composition of alloys, named "ferritic stainless steel," for making low-activation structural materials for fusion reactor [2]. The development of low-activation materials requires a good knowledge of

*Corresponding author, E-mail: gandhiaman653@gmail.com

the excitation functions. The nuclear data for the low-activation materials may be advantageous over evaluating the nuclear parameters like nuclear decay heat (for safety purpose), neutron-induced radioactivity (for waste management) and radiation-effect on the materials (for maintenance of reactors) of the first wall and blanket of fusion reactors [2, 3]. Hence, the accurate experimental measurements and theoretical calculations of the fast neutron-induced reaction cross-sections are essential for such materials for the efficient and pertinent working of the nuclear reactors.

The nuclear data available in the IAEA-EXFOR database for neutron energies up to 30 MeV show that significant experimental data are missing in certain energy range, as well as some discrepancies exist between the different measurements for a number of activation cross-sectional data [4]. Therefore, carrying out the calculations in this energy region would help us to study the energy dependency of the activation cross-sections in detail, thereby gaining a better understanding of the reaction mechanism. So, keeping the above issues as part of motivation, we have calculated the excitation functions for the reactions ^{52}Cr(n,p)^{52}V, ^{52}Cr(n,α)^{49}Ti, ^{52}Cr(n,2n)^{51}Cr, ^{56}Fe(n,p)^{56}Mn, ^{56}Fe(n,α)^{53}Cr, and ^{56}Fe(n,2n)^{55}Fe up to 30 MeV neutron energies, using the nuclear reactions model codes TALYS-1.8 [5, 6] and EMPIRE-3.2.2 [7, 8].

2. Nuclear models and calculations

Nuclear models play an important role in the estimation of the nuclear reaction cross-section and to understand different reaction processes. The model calculations can make a good estimate of the cross-sectional data where the experimental data are not available. For the production of the medical radionuclide, the evaluated nuclear model data are equally important corresponding to the experimental data. The data obtained from the nuclear model codes also have applications related to nuclear reactions for predicting and simulating the reaction cross-section, such as in accelerator-driven system (ADS) for predicting the neutron production rate from the charged-particle-induced reaction on high Z materials and also for the nuclear reactors safety related to the shielding, material damage, activation and radiation heating [9–12]. In this work, the theoretical model calculations have been done using the two computer codes TALYS-1.8 and EMPIRE-3.2.2. These codes provide the complete and precise information about the different mechanisms like direct, pre-compound or pre-equilibrium and compound nucleus processes [6, 8]. These codes help us to predict the cross section of isotopes for which the experimental measurements are not feasible. The reaction mechanisms vary with the incident neutron energy. In the lower energy region, the excitation functions are dominated by the compound nucleus process, while toward higher region, the pre-equilibrium process becomes more active [13]. The energy-dependent level density parameters are important in the statistical model calculations for predicting the cross section at higher excitation energies. For calculating these parameters, different level density models are defined in TALYS-1.8 and EMPIRE-3.2.2 codes, which range from phenomenological models to tabulated level densities, calculated from microscopic models [5, 7]. Here, we present a comparison of the different phenomenological level density models which are used for the calculations of energy-dependent nuclear level density parameters, and the excitation functions results which acquired with the best combination of the reliable nuclear models.

2.1. TALYS-1.8

TALYS is a user-friendly nuclear reaction model code, which is used for the simulation and analysis of the nuclear data for all the open reaction channels induced by light nuclei in the 1 keV–200 MeV incident energy range [5]. In this code, the default local optical model potentials (OMP) have been used for the outgoing protons and neutrons which are parameterized by Koning and Delaroche [14], while for the α-particles, the parameters of Avrigeanu et al. [15] have been adopted. All the optical model (OM) and direct reaction calculations have been performed by ECIS-06 code [16]. The Hauser–Feshbach model has been used for the compound nucleus reaction contribution, and for the pre-equilibrium emission, the two-component exciton model has been used, which considered the neutron or proton types of particles and holes throughout the reaction. For the γ-ray emission, the γ-ray strength function with multi-polarity as described by Kopecky-Uhl generalized Lorentzian model has been used [17]. Both the γ-ray strength function and nuclear level density parameters are used in the statistical model calculations for predicting the cross sections. In this work, the excitation function calculations are carried out using the phenomenological nuclear level density (NLD) models, i.e., Gilbert and Cameron Model (Constant temperature model (CTM) + Fermi gas model (FGM)) [18], the Back-shifted Fermi gas model (BSFG) [19] and Generalized superfluid model (GSM) [20, 21].

For the level density parameter calculations, the energy-dependent level density parameter (a) of Ignatyuk et al. has been used. This parameter is approximated by the following expression [22]:

$$a = \tilde{a}\left(1 + \delta s \frac{1 - \exp[-\gamma U]}{U}\right) \quad (1)$$

where (ã) is the asymptotic value of the level density parameter (a) at high excitation energy U, i.e., ã = $a(E_x \rightarrow \infty)$. γ is the damping parameter which ascertain how rapidly $a(E_x)$ approaches ã. δs is the shell correction energy.

In the Gilbert and Cameron model (ldmodel 1), the constant temperature model (CTM) is used for the low excitation energy region and the Fermi gas model (FGM) is used for the high excitation energy region. In the Fermi gas expression, the effective excitation energy is given by $U = E_x - \Delta_{CTM}$; here, the pairing energy shift (Δ) is given by

$$\Delta_{CTM} = n\frac{12}{\sqrt{A}} \quad (2)$$

where $n = 0$ holds for odd–odd, 1 for odd–even, 2 for even–even nuclei, and A is the atomic number.

In the Back-shifted Fermi gas model (ldmodel 2), the effective excitation energy is given by $U = E_x - \Delta_{BSFG}$, where

$$\Delta_{BSFG} = n\frac{12}{\sqrt{A}} + \delta \quad (3)$$

here, $n = -1$ for odd–odd, 0 for odd–even and 1 for even–even nuclei. δ is the adjustable parameter which is used to fit the experimental data for each nucleus [19].

The Generalized super fluid model (ldmodel 3) considers the superconductive pairing correlations according to the Bardeen–Cooper–Schrieffer (BCS) theory [20, 21]. The effective excitation energy U is defined in the GSM model as $U = E_x - \Delta_{GSM}$ with

$$\Delta_{GSM} = E_{cond} - n\Delta_0 - \delta \quad (4)$$

where $\Delta_0 = \frac{12}{\sqrt{A}}$, E_{cond} is the condensation energy, and n is equal to 0 for even–even, 1 for odd–even, 2 for odd–odd nuclei.

2.2. EMPIRE-3.2.2

EMPIRE is a computer code based on nuclear reaction models which is widely used for the theoretical investigations and nuclear reaction cross-sectional data evaluation over a wide range of incident energies and particles. In EMPIRE-3.2.2, the pre-equilibrium contribution in nuclear reaction cross-sections has been calculated using the phenomenological exciton model (via PCROSS code) that depends on the particle-hole state level densities [23–26]. For the compound nuclear reaction cross-sections, the statistical model based on Hauser–Feshbach formalism has been used. The optical model parameters used in the calculations are taken from the RIPL-3 (Reference Input Parameter Library), in which the parameters proposed by Koning and Delaroche [14] have been used for the outgoing protons and neutrons, whereas the parameters of Avrigeanu et al. [15] have been used for the outgoing α-particles. The gamma-ray strength function described by the modified Lorentzians (MLO1) has been used in the compound nucleus model calculations of particle emission [27]. The parameters used in the model calculation have been retrieved from the RIPL-3 [28]. For the level densities, the default phenomenological level density formalism (LEVDEN 0) known as Enhanced Generalized Superfluid Model (EGSM) has been used in the calculation. In EGSM, below the critical energy U, the nuclear level density is calculated according to GSM, the superfluid model and according to FGM above critical energy [29]. The relation between the effective excitation energy (U) and excitation energy E_x in EGSM model is given as:

$$U = E_x + n\Delta_0 \quad (5)$$

where $\Delta_0 = \frac{12}{\sqrt{A}}$; n = 2, 1 and 0 for odd–odd, odd–even and even–even nuclei, respectively.

The transmission coefficients have been calculated by using the optical model (OM) routines via the ECIS06 code [30, 31], and the spherical optical model calculation has been performed for the direct reaction channel (DIRECT = 0).

3. Results and discussion

In the present study, the excitation functions of (n,p), (n,α), and (n,2n) reactions for $^{52}Cr(n,p)^{52}V$, $^{52}Cr(n,\alpha)^{49}Ti$, $^{52}Cr(n,2n)^{51}Cr$, $^{56}Fe(n,p)^{56}Mn$, $^{56}Fe(n,\alpha)^{53}Cr$, and $^{56}Fe(n,2n)^{55}Fe$ are theoretically calculated with different level density models, optical model potentials and reaction models for neutron energies up to 30 MeV. The results obtained by model calculations are compared with TENDL-2017 [32] and ENDF/B-VIII.0 [33]-evaluated data

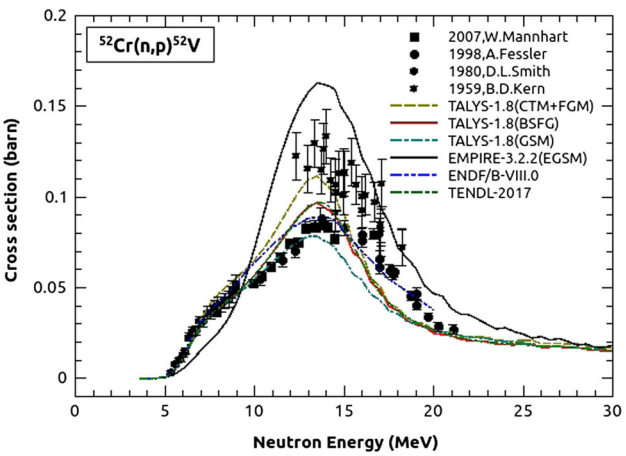

Fig. 1 Excitation functions for $^{52}Cr(n,p)^{52}V$ nuclear reaction

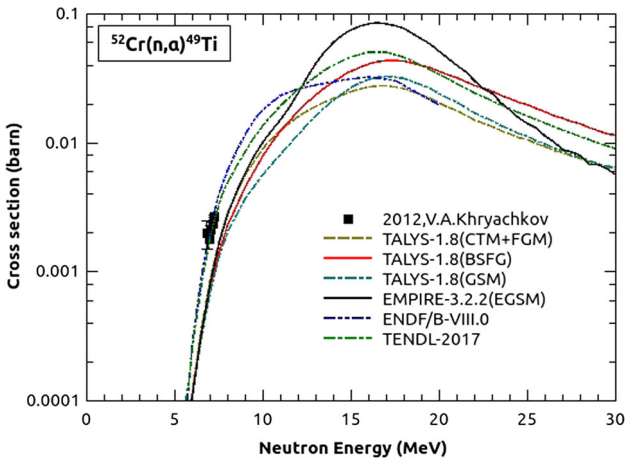

Fig. 2 Excitation functions for $^{52}Cr(n,\alpha)^{49}Ti$ nuclear reaction

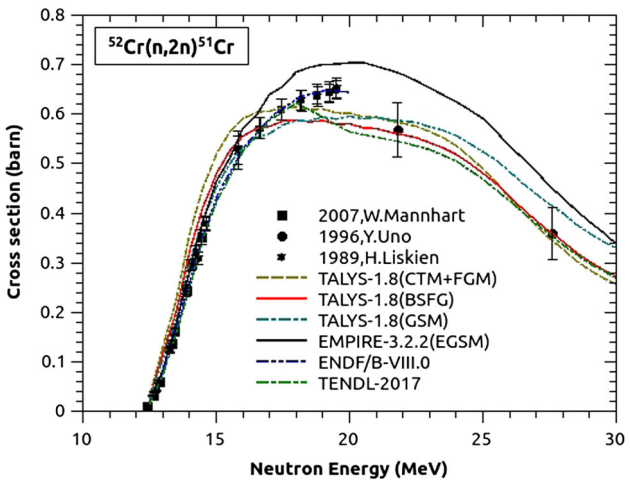

Fig. 3 Excitation functions for $^{52}Cr(n,2n)^{51}Cr$ nuclear reaction

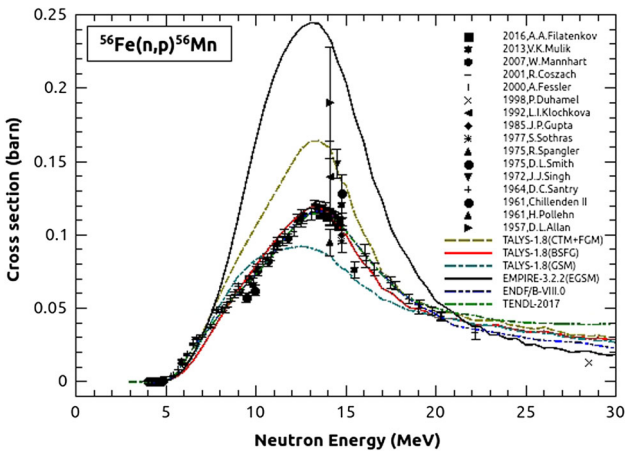

Fig. 4 Excitation functions for $^{56}Fe(n,p)^{56}Mn$ nuclear reaction

as shown in Figs. 1, 2, 3, 4, 5 and 6. The experimental data available in the IAEA-EXFOR database are taken as references for the validation purpose [4].

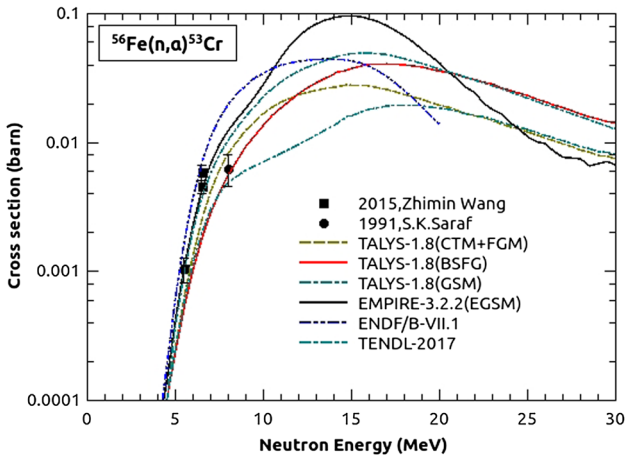

Fig. 5 Excitation functions for $^{56}Fe(n,\alpha)^{53}Cr$ nuclear reaction

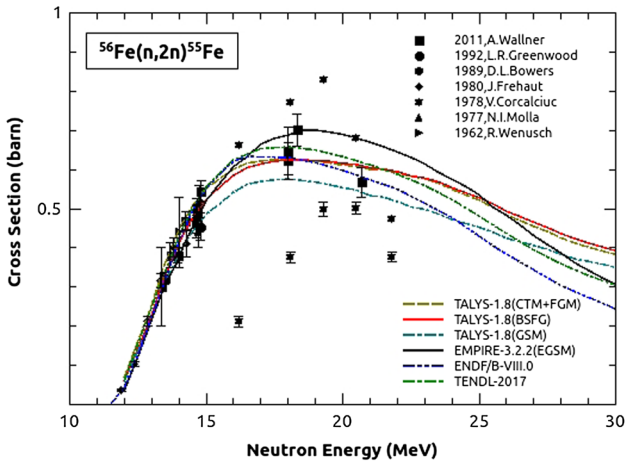

Fig. 6 Excitation functions for $^{56}Fe(n,2n)^{55}Fe$ nuclear reaction

For (n,p), (n,α), and (n,2n) reactions on ^{52}Cr and ^{56}Fe, Q-values and threshold energies are given in the second and third columns of Table 1, respectively, which are taken from the National Nuclear Data Centre (NNDC) [34]. In Table 2, we have listed the level density parameters (a) and the asymptotic level density values (ã) for the residue nucleus which are calculated by the different nuclear level

Table 1 Q-value and threshold energies of (n,p), (n,α), and (n,2n) reaction of ^{52}Cr and ^{56}Fe

Reactions	Q-value (keV)	Threshold (keV)
$^{52}Cr(n,p)^{52}V$	− 3193.13 ± 0.54	3255.15 ± 0.55
$^{52}Cr(n,\alpha)^{49}Ti$	− 1209.05 ± 0.36	1232.53 ± 0.36
$^{52}Cr(n,2n)^{51}Cr$	− 12,039.16 ± 0.51	12,273.01 ± 0.52
$^{56}Fe(n,p)^{56}Mn$	− 2913.19 ± 0.45	2965.74 ± 0.45
$^{56}Fe(n,\alpha)^{53}Cr$	326.32 ± 0.34	0.00 ± 0.00
$^{56}Fe(n,2n)^{55}Fe$	− 11,197.10 ± 0.23	11,399.06 ± 0.23

Table 2 Level density parameters used in the model calculations

NLD model	Nucleus	(a)	($\tilde{a}$)
CTM + FGM	52V	7.36695	7.74006
(ldmodel 1)	49Ti	7.31110	7.16858
	51Cr	6.83789	7.46913
	56Mn	8.34661	8.78571
	53Cr	6.45133	7.11382
	55Fe	6.22374	8.04407
BSFG	52V	6.66361	6.97317
(ldmodel 2)	49Ti	6.00652	5.90433
	51Cr	5.65368	6.10697
	56Mn	7.15091	7.48115
	53Cr	5.20851	5.65620
	55Fe	5.26002	6.51729
GSM	52V	6.43767	6.43767
(ldmodel 3)	49Ti	5.87441	5.87441
	51Cr	5.38703	5.38703
	56Mn	6.81457	6.81457
	53Cr	5.08128	5.08128
	55Fe	4.86788	4.86788
EGSM	52V	3.9881	4.00824
(LEVDEN 0)	49Ti	4.2343	4.25442
	51Cr	4.1650	3.86645
	56Mn	4.5028	4.50327
	53Cr	3.9774	3.95106
	55Fe	3.7675	3.61608

density (NLD) models. The detailed information about our calculations and comparisons for all the reactions is given below.

3.1. ^{52}Cr(n,p)^{52}V reaction

The calculated excitation functions and experimental data for the ^{52}Cr(n,p)^{52}V nuclear reaction are plotted in Fig. 1. The experimental data reported by Mannhart et al. [35], Fessler et al. [36], and Smith et al. [37] at energies 5–10 MeV exhibit the same trend as the excitation functions obtained from the TENDL-2017 and ENDF/B-VIII.0-evaluated data and similar to the results calculated with the BSFG and GSM level density models in TALYS-1.8 code. The experimental data at 10–13 MeV energy range are in good agreement with the excitation curve calculated by GSM model. Furthermore, the cross-sectional data reported by Kern et al. [38] at energies 12–18.5 MeV have a higher value than those of the other measured data, and the theoretically estimated excitation functions are not in agreement. In this maximum cross-sectional region, the excitation functions acquired by the EGSM and CTM + FGM level density models produce higher cross-sectional results. Figure 1 shows the variation of the cross section with the neutron energy. In the lower energy region, the reaction cross-section increases with the neutron energy and then after a particular energy, it starts to fall down due to the opening of another reaction channels like inelastic scattering. The lower energy part of excitation functions is dominated by the compound nucleus process and the pre-equilibrium process occurs at only around 15–30 MeV.

3.2. ^{52}Cr(n,α)^{49}Ti reaction

The excitation functions estimated by the theoretical model codes for the ^{52}Cr(n,α)^{49}Ti reaction are shown in Fig. 2. The excitation curves of the TENDL-2017 and ENDF/B-VIII.0-evaluated data are in good agreement with the existing data at energies 6.5–7.5 MeV, which is reported by Khryachkov et al. [39]. However, the theoretically calculated excitation curves underestimate the experimental data points.

3.3. ^{52}Cr(n,2n)^{51}Cr reaction

The theoretically calculated and the existing experimental data for ^{52}Cr(n,2n)^{51}Cr reaction are shown in Fig. 3. The experimental points of Mannhart et al. [35] and Liskien et al. [40] at energies of 12–15 MeV are in agreement with the TENDL-2017 and ENDF/B-VIII.0-evaluated data and also with the results obtained by the EGSM level densities via EMPIRE code. In addition, the two data points reported by Uno et al. [41] at energies of 21.8 MeV and 27.6 MeV are in agreement with the TENDL-2017 evaluated data, and results obtained from the CTM + FGM, BSFG, and GSM models within the experimental uncertainties. The excitation functions obtained from the ENDF/B-VIII.0-evaluated data have a good match with the experimental data of Liskien et al. [40] in the neutron energy range 15–20 MeV. It is observed from Fig. 3 that the excitation functions calculated by different level density models via TALYS-1.8 and EMPIRE-3.2.2 codes are compatible with each other in the defined nuclear energy region. The fall-down of the excitation curve after the 20 MeV neutron energy marks the increase in pre-compound contribution in the total reaction cross-section.

3.4. ^{56}Fe(n,p)^{56}Mn reaction

The excitation functions of the ^{56}Fe(n,p)^{56}Mn reaction from its threshold value to 30 MeV neutron energies are shown in Fig. 4. The experimental cross-sectional data of ^{56}Fe(n,p)^{56}Mn at energies up to 20 MeV [42–49] exhibit a trend similar to that of the TENDL-2017 and ENDF/B-VIII.0-evaluated data, and similar to the results obtained

using the BSFG level density model in TALYS code. The cross-sectional data at neutron energies up to 8 MeV are consistent with the results estimated by EGSM, CTM + FGM, and GSM models. Furthermore, the excitation curve of CTM + FGM shows a good agreement with the experimental data reported by Allan et al. [50], Singh et al. [51] and Chittenden II et al. [52] in the 14–15 energy range within the data error-bars. In addition, the cross-sectional data of Coszach et al. [53] at 22.2 MeV show good agreement with the cross section obtained from ENDF/B-VIII.0 and BSFG, GSM, and EGSM level density models within the experimental uncertainties.

3.5. ^{56}Fe(n,α)^{53}Cr reaction

The theoretically calculated excitation functions for the fast neutron-induced ^{56}Fe(n,α)^{53}Cr reaction are shown in Fig. 5 with the existing experimental data obtained from the EXFOR database. The data points, at energies 5.5–6.5 MeV reported by Wang et al. [54], are consistent with the TENDL-2017 and ENDF/B-VII.1 evaluations, and results were obtained from the EGSM level density model. The cross-sectional value reported by Saraf et al. [55] at energy 8 MeV is in agreement with the CTM + FGM, BSFG, and GSM models within the experimental uncertainties.

3.6. ^{56}Fe(n,2n)^{55}Fe reaction

The comparison between the theoretically calculated excitation functions and the experimental cross-sectional data for the ^{56}Fe(n,2n)^{55}Fe reaction is shown in Fig. 6. The experimental data points in the 12–15 MeV region show consistency with the excitation functions obtained from the evaluated nuclear data files and the theoretically estimated cross sections within the data error-bars [56–61]. The excitation functions obtained from the CTM + FGM, BSFG, and GSM models and ENDF/B-VIII.0 evaluations agree with the cross-sectional data at 18 MeV and 20.68 MeV, reported by Wallner et al. [56]. The data reported by Corcalciuc et al. [62] in the 16–22 MeV neutron energy range indicate discrepancies in their experimental values, and the model calculated results are not in agreement with the experimental data. However, the experimental data at 18.33 MeV and 20.5 MeV energies reported by [56, 62] show good agreement with the excitation functions, calculated by the EGSM level density model. This evaluation results of the excitation function for the ^{56}Fe(n,2n)^{55}Fe reaction can be important for improving the theoretical models, which are based on the phenomenological optical parameters in order to provide a reliable estimation of the cross section.

4. Conclusions

The theoretical calculations of the excitation functions for the fast neutron-induced reactions on ^{52}Cr and ^{56}Fe isotopes have been studied using the TALYS-1.8 and EMPIRE-3.2.2 computer codes. The influence of nuclear level density models on the calculated excitation functions has been analyzed for the desired nuclear reactions. The results show that the excitation functions are strongly dependent on the selection of reliable nuclear level density models for obtaining the accurate results. The bump of the excitation functions in 10–20 MeV neutron energy region as shown in Figs. 1, 2, 3, 4, 5 and 6 indicates about the increasing contribution of the pre-equilibrium process. The contribution of the direct reaction process is negligible in comparison with the compound nucleus contribution in the reaction total cross-section. There is no experimental data for the ^{56}Fe(n,α)^{53}Cr and ^{52}Cr(n,α)^{49}Ti reactions in the 8–30 MeV neutron energy region which can validate the theoretically calculated results. To solve these discrepancies, there is a need for new precise experimental measurements for these two reactions in the above specific fast neutron energy region. The evaluated excitation functions in the selected neutron energy range can be useful for the fusion reactor technology.

Acknowledgements One of the authors (A. Kumar) thanks to the DAE-BRNS, Government of India (Sanction No. 36(6)/14/23/2016-BRNS), IUAC-UGC, Government of India (Sanction No. IUAC/XIII.7/UFR-58310) and DST, Government of India (Sanction No. INT/RUS/RFBR/P-250) for the financial support for this work.

References

[1] P Reimer *PhD Thesis* (University of Cologne) (2002)
[2] E E Bloom et al. *J. Nuclear Mater.* **122** 17–26 (1984)
[3] R A Forrest and G J Butterworth *Nuclear Data for Science and Technology, Springer* (Berlin, Heidelberg) p 267–272 (1992)
[4] IAEA Experimental Nuclear Reaction Data (EXFOR) https://www-nds.iaea.org/exfor/exfor.htm
[5] A Koning, S Hilaire, and S Goriely TALYS-1.8 manual http://www.talys.eu/download-talys/.talys1.8.pdf (2015)
[6] TALYS-1.8 software for simulation of nuclear reactions http://www.talys.eu/download-talys/
[7] M Herman et al. *Nuclear Data Sheets* **108** 2655 (2007)
[8] EMPIRE-3.2.2 system of codes for nuclear reaction https://www.nds.iaea.org/index-meeting-crp/EmpireWorkshop2013/downloadEmpire322win.htm
[9] M Sadeghi and M Enferadi *Ann. Nuclear Energy* **38** 825–834 (2011)
[10] M Sadeghi, M Enferadi, and H Nadi *J. Radioanal. Nuclear Chem.* **286** 259–263 (2010)
[11] M Sadeghi, N Soheibi, T Kakavand, and M Yarmohammadi *J. Radioanal. Nuclear Chem.* **293** 1–6 (2012)
[12] M Sadeghi, M Enferadi, H Nadi, and C Tenreiro *J. Radioanal. Nuclear Chem.* **286** 141–144 (2010)
[13] B Lalremruata et al. *Ann. Nuclear Energy* **36** 458–463 (2009)

[14] A J Koning and J P Delaroche *Nucl. Phys. A* **713** 231–310 (2013)
[15] V Avrigeanu, M Avrigeanu, and C Manailescu *Phys. Rev. C* **90** 044612 (2014)
[16] J Raynal *CEA Saclay Report No CEA-N-2772* (1994)
[17] J Kopecky and M Uhl *Phys. Rev. C* **41** 1941 (1990)
[18] A Gilbert and A G W Cameron *Can. J. Phys.* **43** 1446 (1965)
[19] W Dilg, W Schantl, H Vonach, and M Uhl *Nucl. Phys. A* **217** 269 (1973)
[20] A V Ignatyuk, K K Istekov, and G N Smirenkin *Sov. J. Nucl. Phys.* **29** 450 (1979)
[21] A V Ignatyuk, J L Weil, S Raman, and S Kahane *Phys. Rev. C* **47** 1504 (1993)
[22] A V Ignatyuk, G N Smirenkin, and A S Tishin *Sov. J. Nucl. Phys.* **21** 255 (1975)
[23] J J Griffin *Phys. Rev. Lett.* **17** 478 (1966)
[24] C K Cline and M Blann *Nucl. Phys. A* **172** 225 (1971)
[25] C K Cline *Nucl. Phys. A* **193** 417 (1972)
[26] I Ribanský, P Obložinský, and E Bětak *Nucl. Phys. A* **205** 545 (1973)
[27] V A Plujko *Acta Phys. Pol. B* **31** 435 (2000)
[28] R Capote et al. *Nuclear Data Sheets* **110** 3107 (2009)
[29] A D'Arrigo et al. *J. Phys. G.* **20** 365 (1994)
[30] J Raynal, *Technical Report No. SMR-9/8 IAEA* (unpublished)
[31] J Raynal *ICTP International Seminar Course* (IAEA, ICTP, Trieste, Italy) p. 281 (1972)
[32] Talys Evaluated nuclear data libraries https://tendl.web.psi.ch/tendl-2017/tendl2017.htm
[33] Evaluated nuclear data files https://www.nds.iaea.org/exfor/endf.htm
[34] NNDC https://www.nndc.bnl.gov/qcalc/
[35] W Mannhart and D Schmidt *No. PTB-N–53, Physikalisch-Technische Bundesanstalt* (2007)
[36] A Fessler, E Wattecamps, D L Smith, and S M Qaim *Phys. Rev. C* **58** 996 (1998)
[37] D L Smith and J W Meadows *Nuclear Sci. Eng.* **76** 43–48 (1980)
[38] B D Kern, W E Thompson, and J M Ferguson *Nucl. Phys.* **10** 226–234 (1959)
[39] V A Khryachkov et al. *EPJ Web of Conferences* ***21*** (2012)
[40] H Liskien, M Uhl, M Wagner, and G Winkler *Ann. Nuclear Energy* **16** 563–570 (1989)
[41] Y Uno et al. *Nuclear Sci. Eng.* **122** 247–257 (1996)
[42] A A Filatenkov *USSR report to the INDC 0460* (2016)
[43] A Fessler et al. *Nuclear Sci. Eng.* **134** 171–200 (2000)
[44] D Paul et al. *Nuclear Instrum. Methods Phys. Res. Sect. A* **404** 143–148 (1998)
[45] L I Klochkova, B S Kovrigin, and V N Kuritsin *No. INDC (CCP)-376, IAEA* (1994)
[46] J P Gupta, H D Bhardwaj, and R Prasad *Pramana* **24** 637–642 (1985)
[47] S L Sothras *PhD Thesis* (University Microfilms Order No. 78-09,993, United States) (1977)
[48] R Spangler, E L Draper, and T A Parish (Univ. of Texas, Austin) (1975)
[49] D L Smith and J W Meadows *Nuclear Sci. Eng.* **58** 314–320 (1975)
[50] D L Allan *Proc. Phys. Soc. Sect. A* **70** 195 (1957)
[51] J J Singh *Trans. Am. Nucl. Soc* **15**:147–148 (1972)
[52] D M Chittenden II, D G Gardner, and R W Fink *Phys. Rev.* **122** 860 (1961)
[53] R Coszach et al. *Phys. Rev. C* **61** 064615 (2000)
[54] Z Wang et al. *Phys. Rev. C* **92** 044601 (2015)
[55] S K Saraf et al. *Nuclear Sci. Eng.* **107** 356–373 (1991)
[56] A Wallner et al. *J. Kor. Phys. Soc.* **59** 1378 (2011)
[57] L R Greenwood *No. Conf-8909234–1, Argonne National Lab.* (USA) (1989)
[58] D L Bowers and L R Greenwood *J. Radioanal. Nuclear Chem.* **123** 461–469 (1988)
[59] Joel Frehaut et al. *No.CEA-CONF–5486, CEA Centre d'Etudes de Bruyeres-le-Chatel* (1980)
[60] N I Molla and S M Qaim *Nucl. Phys. A* **283** 269–288 (1977)
[61] R Wenusch and H Vonach *J. Oesterr. Akad. Wiss. Math. Nat.* **99** 6201 (1962)
[62] V Corcalciuc et al. *Nucl. Phys. A* **307** 445–471 (1978)